Research & Reviews: Journal of Engineering and Technology

e-ISSN:2319-9873

Effect of Carbon Content onto Silicon-Carbon Alloys Properties Elaborated For The Passivation of Monocrystalline Solar Cell

Salwa Merazga*, Aissa Keffous, Abdelhak Cheriet, Khadidja Khaldi, Michel Rosso, Mohamed Kechouane and Noureddine Gabouze

[1]Research Center Semiconductor Technology for Energetic, 02 Bd, Frantz FANON, Algiers, Algeria

[2]Laboratory of Materials Physics, USTHB, BP 32 El Alia, Algiers, Algeria

[3]Laboratory of Condensed Matter Physics (PMC). Joint Research Unit 7643 du CNRS et de Ecole Polytechnique, 91128 Palaiseau cedex, France

Review Article

Received date: 19/03/2018

Accepted date: 30/04/2018

Published date: 30/05/2018

***For Correspondence**

Salwa Merazga, Research Centre Semiconductor Technology for Energetic, 02 Bd,Frantz FANON, B.P. 140, Algiers,Algeria, Tel: +213550521031.

E-mail: merazgasal@yahoo.fr

Keywords: Plasma enhancedchemical vapour deposition process, Silicon-carbon, Passivation, Solar cell

ABSTRACT

A hydrogenated amorphous silicon-carbon alloys thin films have been grown at low power regime via plasma enhanced chemical vapour deposition process (PECVD) with decomposition of silane (SiH_4) and methane (CH_4) at varying carbon content (x). The carbon content is restricted to the range $0<x<0.3$. The structural properties of the thin films were investigated using infrared spectroscopy (FTIR), secondary ion mass spectrometry (SIMS), scanning electronic microscopy with elementary chemical analysis

(EDAX) and atomic force microscopy techniques. In addition, the optical properties were studied by UV-visible-NIR spectrophotometry and current–temperature measurements (I (T)), respectively. The optical gap (E_g) can then reach high values, allowing electroluminescent devices emitting visible light. Nevertheless, the Si–C network is not allowed to relax to the more stable sp^2–sp^3 admixture; this material is more stressed than the low-gap standard material. The better passivation is obtained to low levels of carbon; the effective life time reaches a value of 121 μs for 5% carbon.ments.

Hence in the present investigation attempts have been made on the following major sections fuel manifold design substantiation for temperature and pressure requirement, vibration analysis, high cycle and low cycle fatigue analysis, design optimization using additive manufacturing technique. A comparative study has been made between conventional and additive manufacturing. Analysis results has been correlated based on hand calculated results which indicates less than five percent deviation to satisfy the FAA guidelines.

The rise in number of vehicles had led to many problems like traffic congestion, increase in consumption of fuels, rising travel costs. Considering all these problems we have studied different papers. This paper introduces bike sharing application which will help people to travel on one bike and share their expenses and also reduce pollution.

INTRODUCTION

Hydrogenated amorphous silicon carbide is a very promising material for a number of applications such as optoelectronic devices, solar cells [1] light emitting diodes [2], sensors [3] et transistors (TFT) [4]. All these applications are based on exclusive properties of these thin films, such as the wide bandgap, adjustable index, high electron mobility and high thermal conductivity. The magnitude of this material offered from the fact that its electrical and optical properties can be controlled by varying the carbon, silicon, and hydrogen composition of this alloys.

These films can be deposited by different techniques such as magnetron sputtering [5] and Plasma enhanced chemical vapor deposition (PECVD) [6]. However, the PECVD is the most widely used due to its ability to produce high quality thin films with good physical and electronic properties at low substrate temperature. Various studies have been developed for better understanding and control of material properties depending on the deposition conditions [7-9].

Solomon I has been shown that a high optical gap, with a record value of 3.7 eV for a-Si1$_{-x}$(CH3)$_x$:H thin films containing 42% of carbon deposited by RF-PECVD technique [10]. Recently, Touahir A et al. have reported that concentration of Carbone (x) up to 0.2, the Carbone is mostly inserted as methyl groups (CH_3) in the amorphous methylated silicon a-Si1$_{-x}$(CH_3)$_x$:H thin films prepared by PECVD from SiH_4 [11].

In this paper, we reported the results of the characterized a-Si1$_{-x}$(CH_3)$_x$:H thin films prepared at different Carbone concentration, by a RF-PECVD technique. This deposited films have been characterized by: Elementary chemical analysis (EDAX), atomic force microscopy (AFM), secondary ion mass spectrometry (SIMS), Fourier transform-infrared spectroscopy (FTIR), I(T) measurement, were used in order to characterize the deposited films. The influence of carbon concentration on the structural, optical and electrical properties was investigated. The influence of carbon concentration on the structural, optical and electrical properties of the deposited a-S$_i$1-x(CH_3)x:H thin films were investigated.

EXPERIMENTAL DETAILS

Intrinsic hydrogenated silicon- carbon alloys (a-Si1$_{-x}$(CH_3)$_x$:H) thin films were deposited simultaneously on Corning 7059 glass and c-Si(p) wafers (111) by radio frequency (13.56 MHz) plasma enhanced chemical vapor deposition (RF-PECVD) system in a "low-power" regime of 10W [12] with SiH_4 and CH_4 gas mixture at 250°C, and the working pressure was fixed to 40 mTorr. Different layers of a-Si1-x(CH_3)x:H were prepared by PECVD in the low-power regime by varying carbon content (x=0.05, x=0.10, x=0.15 and x=0.20). Moreover, the carbon content (x) calculated by varying the methane ratio in the gas mixture ([CH_4] / [S_iH_4] + [CH_4]) as proposed by Solomon I et al. [13]. Carbon content in the film was controlled through the gas-phase composition, i.e., [CH_4] partial pressure in the [CH_4] / [S_iH_4] mixture [11]. The investigated carbon content (x) were x = 0.05, x = 0.10, x = 0.15 and x = 0.20. During film deposition, the substrate temperature was maintained at 250 °C. Before a-Si1$_{-x}$(CH_3)$_x$:H deposition, c-Si wafers and Corning substrate were cleaned in a H_2SO_4+H_2O_2 (3:1) mixture for 10 min, dipped in 5% HF for the c-Si wafers only for 10 s etches away 4any native oxide grown on the wafer surface and immediately introduced into the PECVD reactor. The parameters of deposition are listed in **Table 1.** The structural properties Fourier transform-infrared (FTIR) absorption measurements were carried by using infrared spectroscopy (Perkin Elmer), Secondary ion mass spectrometry (SIMS) measurements were carried out by means of an Cameca IMS 4FE$_7$ mass spectrometer (CRTSE-Algiers) to determine the carbon fraction x. The morphology of films surface was examined by atomic force microscopy (AFM) using the contact mode JSPM 5200 (USTO-Oran). The optical band gap (Eopt.) of the a-SiC:H was deduced from the transmittance spectra of the films deposited on a glass substrate using a UV-visible spectrophotometry in the range of 300 - 2500nm by Varian Cary 500 (CRTSE-Algiers) whereas the thickness of this films were calculated by the spectroscopic Ellipsometry Analyser Semilab (SEA) (LPM / U.S.T.H.B-Algiers) at wavelength 632.8 nm. The I(T) measurements were measured in a coplanar configuration using Keithley 617 electrometer. Film conductivity as a function of the temperature was measured from room temperature to about 400 K, in high vacuum, at a pressure <10^{-5} mbar (LPM / U.S.T.H.B-Algiers).

Sample	Carbon content	% CH_4	% SiH_4	CH_4 (sccm)	SiH_4 (sccm)
E1	0,20	80	20	26,5	6,6
E2	0,15	74	26	24,6	8,6
E3	0,10	63	37	20,9	12,3
E4	0,5	40	60	13,3	20

Table 1. Parameters of studied thin a-Si1-x(CH_3)x:H films.

RESULTS AND DISCUSSION

Structural Properties

Infrared fourier transform spectroscopy

Figure 1 presents the infrared spectra for bare silicon, as reference and as-deposited amorphous films at different carbon concentration (x=0.05, 0.10, 0.15, 0.20) in the range of 600 - 3000 cm^{-1}. This spectra show seven main absorption bands at 630 cm^{-1}, 780 cm^{-1}, 1100 cm^{-1}, 1230 cm-1, 1400 cm^{-1}, 1590 cm^{-1}, 2820 cm^{-1}, 2890 cm^{-1}. A change in the form of the spectrum with increasing carbon concentration has been observed in the film. Indeed, it shows that the intensity of the band around 630 cm^{-1} related to the Si-H_2 wagging vibration mode, when the intensity of this band decreases with the carbon concentration as shows on **Figure 1**. In addition, the peak at 780 cm^{-1} assigned to the stretching mode of Si-C increases in intensity with the increase of carbon quantity in the film [14,15]. But, the growth of second band of S_iC around 1100 cm^{-1} confirms the incorporation of the carbon in the form of methyl groups [16].

e-ISSN:2319-9873

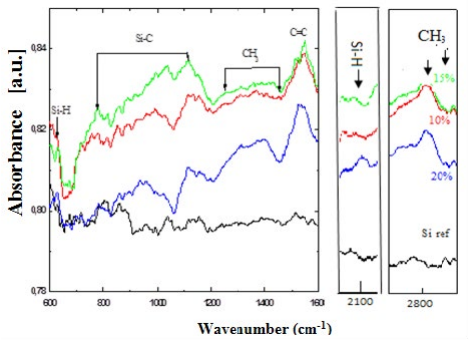

Figure 1. Infrared spectrum of thin a-S_i1-x(CH_3)x:H films at different carbon content (x).

A special area around 1200-1500 cm^{-1} characteristic modes of Si-CH_3 which are symmetric mode from 1235 to 1280 cm^{-1} which correspond an anti-symmetric mode at 1400 cm^{-1} [17-19]. The band around 780 cm^{-1} correspond to the stretching mode of the intense S_iC bond of the sample prepared at 15% carbon. A peak around 1590 cm^{-1} correspond to the aromatic stretching of C=C bonds carbon [18]. With an intensity that increases with the in-crease of carbon concentration.

In the region of 2800-3000 cm^{-1}, two bands appeared around 2820 cm^{-1} corresponds to the symmetric mode of CH_3 bond [17]. In contrast, the peak corresponds to the Si-H stretching at 2010 cm^{-1} for x=0.10-0.15 and 2080 cm^{-1} for x=0.20.

A modification of spectrum shape with the increasing of carbon concentration in the layer was observed. All the carbon bonds (C=C, Si-CH_3 and CH_3) increase substantially in intensity with increasing the amount of carbon in the layer. This result is expected view that increasing the amount of carbon promotes the formation of carbon bonds at the other bonds. Indeed, the intensity of the band around 2000 cm^{-1} changes its position with increasing concentration atoms. This shift already reported in the literature [17]. Suggests its assignment to the appearance of around Nano vides. In this case, it can be expected that the carbon is incorporated in the material, as a coordinated atom with an atom of Si (S_i-C) whether is coordinated with a single atom of silicone and three hydrogen atoms (Si-CH_3) or three atoms hydrogen (CH_3). Overall, the data of infrared confirm the incorporation of carbon such as methyl groups [17].

Secondary ion mass spectrometry (SIMS)

We have used a dynamic SIMS to determine the concentration of the various constituents of the alloy S_i-C. The carbon content (x) in thin a-S_i1-x(CH_3)x:H film has been mentioned **(Table 2)**. **Figure 2** presents the evolution of the carbon and the hydrogen concentration present in the Si-C alloy as a function of carbon content. Where we can see, that the concentration of hydrogen is higher than the carbon one, result which is corroborated by the presence of hydrogen in SiH_4 and CH_4 and to incorporate the H atoms to form an alloy S_i-C as a-S_i1-x(CH_3)x:H, the concentration decreases in the same order then increases to reach an optimum value corresponding to 2.0 10^{22} and 3.8 10^{22} at/cm^3 for carbon and hydrogen, respectively.

Table 2. Stoichiometry of thin a-Si1-x(CH_3)x:H films.

Sample	Carbon content	[Si]/[C]+[Si]	Alloy Structure a-Si1-x(CH_3)x:H	^{12}C (at/cm_3)	^{1}H (at/cm_3)
E1	0.20	0.92	a-Si0.92(CH3)0.08:H	6 1021	1,7 1022
E2	0.15	0.86	a-Si0.86(CH3)0.14:H	2,2 1022	3,8 1022
E3	0.10	0.66	a-Si0.66(CH3)0.34:H	1,8 1022	2,3 1022
E4	0.05	0.88	a-Si0.88(CH3)0.34:H	3 1022	2,9 1022

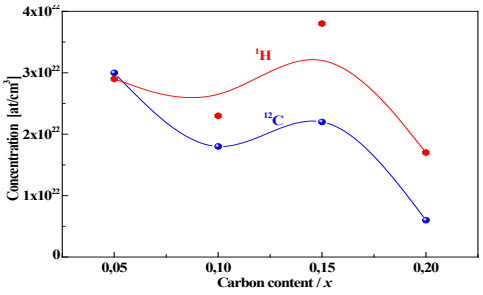

Figure 2. The evolution of the carbon and the hydrogen concentration present in the Si-C.

Energy dispersive x-ray spectroscopy (EDAX)

Using the Energy Dispersive X-Ray Spectroscopy (EDAX) extends the usefulness of SEM in that elemental analysis can be performed within regions as small as a 3 μm. This analysis consists in the interaction between an electron beam and the sample end the intensities of the signal depends on the nature of the sample. All elements from boron through the periodic table can be detected with sensitivities of approximately a few tenths of one percent, when the atomic concentrations of the various constituents (Si, C) of the compound are determinate. In the **Figure 3**, the apparently high signal of Si (75.34%) and (24.66%) of C of a-S_i1-x(CH_3)x:H (x=0.2) sample; even the H is not detectable element by the SEM-EDAX. These results confirmed our experiment conditions, where we used a concentration of 20% de carbon.

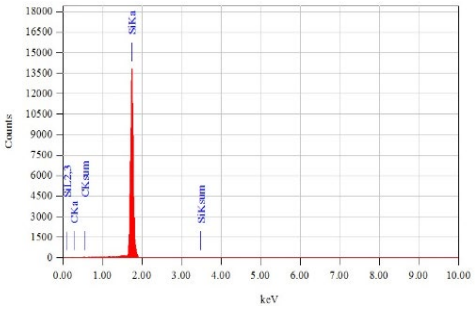

Figure 3. Contact mode AFM images of the as-deposited sample of x=0.20.

Atomic force microscope (AFM)

Atomic Force Microscope (AFM) is a very versatile instrument to study the topography of the sample. The AFM images were acquired by using the contact mode AFM system at room temperature. **Figure 4** shows AFM image of the surface morphology of the as deposited a-S_i1-x(CH_3)x:H sample (80% CH_4). It was found a smooth surface over an area of 10 μm × 10 μm with appearance of a defect on the surface due to a formation of clusters although of the films deposition.

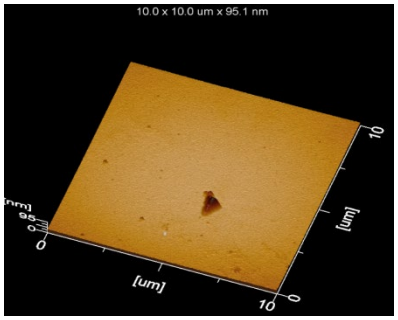

Figure 4. EDAX spectrum of thin a-S_i1-x(CH_3)x:H for x=0.20.

OPTICAL PROPERTIES

We measured the optical property, such as band gap energy (Eg), the refractive index (n) and the thickness by spectroscopic ellipsometry of Semilab-Spectoscopic Ellipsometry Analyser (SEA), in the range 200-900nm. **Figure 5** depicts the variation of Eg (5a) and the Thickness (5b) of a-S_i1-x(CH_3)x:H thin films as a function of carbon content (x). The band gap (Eg) of the a-Si_1-x(CH_3) x:H thin films increases continually with the with the increase of carbon content, reaches a maximum value 2.4 eV for x=0.15, this result was reported by several authors [20-22]. It suggested that to enhance sp^3 bond, the radicals are increased with the carbon content. Indeed, the carbon atom is smaller than a silicon atom; the Si-C bond is shorter than the Si-Si. These results in increased interaction between the atoms, an increase in the energy of optical gap Eg was noticed. In particular, the low value of the maximum band-gap found at x=0.15 by most authors can only be explained by the presence of a certain proportion of sp^2 hybrids resulting in a lowering of the gap by graphitic bonds. The sp^2 sites forming p-bonded clusters, as the carbon concentration increases, tends to stabilize the alloys and to relax the amorphous network by decreasing the tetrahedral coordination and adding some medium-range order to the normal sp^3 short range order, in practice, most of the S_iC amorphous alloys, whatever the method of preparation, contain a variable amount of sp^2 and sp^3 concentrations, resulting in a wide range of properties [21,22].

The **Table 3** resume the optical parameters of the deposited thin a-S_i1-x(CH_3)x:H films.

e-ISSN:2319-9873

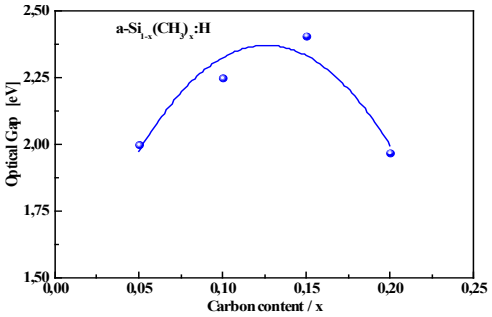

Figure 5. Optical gap variation functions of carbon content (x).

Table 3. Optical parameters of thin a-Si1-x(CH_3)x:H films.

Sample	Carbon content	Thickness [nm]	n	Eg [eV]
E1	0.20	51.1	1.57	1.97
E2	0.15	29.4	2.62	2.41
E3	0.10	74.8	2.18	2.25
E4	0.05	43.6	1.45	2.00

PHOTOCONDUCTIVITY MEASUREMENTS

Figure 6 presents the variation of the dark conductivity (σd) a photoconductivity (σph) versus temperature in Arrhenius plot. This electrical parameter increases exponentially with the measured temperature, according to the equation:

$$\sigma(T) = \sigma 0 \exp(-\frac{Ea}{kT})$$

Where, $\sigma 0$ is the 'minimum conductivity'; k, the Boltzmann's constant Ea, the conductivity activation energy.

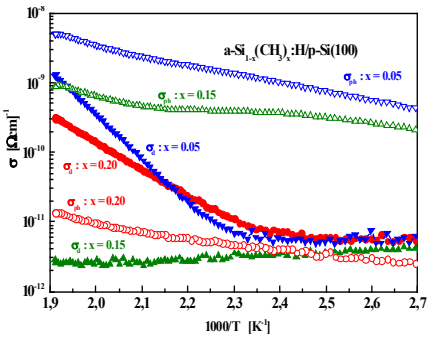

Figure 6. The variation of the dark conductivity (σd) a photoconductivity (σph) versus temperature in Arrhenius plot

The dark conductivity shows a linear variation, this variation indicates that the conduction in our movies is thermally activated. Both quantities exhibit a significant variation with decrease in carbon content. When, the samples with 5% C have the best values of the dark conductivity and the photoconductivity between 10^{-9} - 10^{-12} Ω^{-1} cm^{-1} and 10^{-10} - 10^{-9} Ω^{-1} cm^{-1} respectively. Also **Figure 7** shows the room temperature dark and photoconductivity, as a function of the carbon contents in the range from 0.05 to 0.2. The present σd and σph data for various carbon contents can be broadly divided into two distinct variations: For the dark conductivity (σd), the values of σd are found to tend to be constant for all the carbon content. Thereafter, for the photoconductivity (σph) it increases significantly with the increases of carbon content, where the order of magnitude of this increase seems more important for the films prepared at high carbon content. Therefore, the defect density increases with the decrease of the carbon concentration (C%) et becomes a pinning center of the charge carriers which is directly affects the conductivity of the material.

e-ISSN:2319-9873

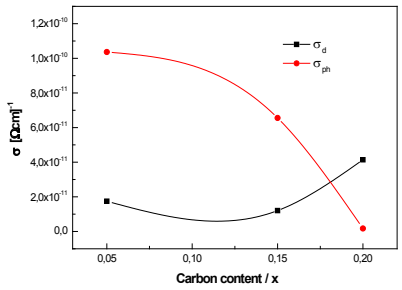

Figure 7. Dark and photoconductivity versus temperature.

C-Si SURFACE PASSIVATION WITH a-Si1-x(CH_3)x:H THIN FILMS

The effective lifetime of carriers was measured by the Quasi-Steady photo conductance state technique (QSSPC). This measures have been performed on n-type silicon wafers (CZ polished surfaces,1-10 Ωcm resistivity) on which the RF-PECVD a-Si1-x (CH_3) x: H was carried out on both faces of the substrate varying the concentration of atoms, applying the following procedure: CZ c-Si wafers (1-10 Ω.cm) were cleaned in a H_2SO_4+H_2O_2 (3:1),dipped in 5% HF, dried immediately introduced into the PECVD reactor where a-Si1-x (CH_3) x:H layers with thickness in the range of 50 nm were sequentially deposited on both surfaces [23]. In **Figure 8**, we present the variation of the lifetime of minority carriers in function of the concentration of carbon for a 10^{15} at/cm^3 correspond to 1 sun. We see that the life time of minority carriers decreases with increasing of the carbon concentration, where its reaches a value of 121 × 10^{-6} s for 5% carbon and does not exceed to the value 6.5 µs for a layer of 20% carbon. Consequently, a better passivation is obtained to low levels of carbon; our results are in agreement with those obtained by Gaufres A et al. [24]. Where, they found that the defect density increases with increasing concentration carbon (C %). This increase in the carbon content results by a decrease of Si-Si and Si-H.

The hydrogen atoms contained in the silicon which are responsible for the saturation of the surface dangling bonds will be replaced by carbon atoms. Therefore, a reduction in the passivation is noticed. Thereafter, we deposited a layer with 5% carbon on the both faces of a solar cell n^+/p. The measurement of the lifetime of the layers deposited on this solar cell has been done in **Figure 9**. This **Figure 9** shows the evolution of the life time according to the density of minority carriers injected from in the mono crystalline solar cell (n^+p), in the presence of a passivation layer of a-Si1-x(CH_3)x:H (5% C). But, we noted that the lifetime does not exceed a value of 50 × 10^{-6} s for a level of injection of 8.10^{15} cm^{-3}.

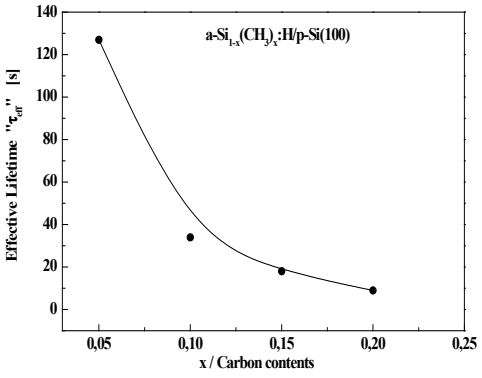

Figure 8. Effective life time versus density minority carriers.

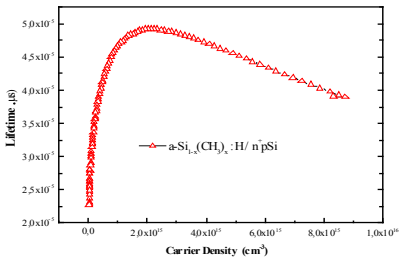

Figure 9. Effective life time function of carbon content (x).

CONCLUSION

In a conclusion, a carbon is incorporated as methyl groups $-CH_3$, thus forcing sp^3 hybridization in the solid to elaborate an amorphous Si-C alloy. The optical gap (Eg) can then reach high values, allowing electroluminescent devices emitting visible light. In the Si-C alloy, which it shows that a low value of the maximum band-gap found at x= 0.15 by most authors can only be explained by the presence of a certain proportion of sp^2 hybrids resulting in a lowering of the gap by graphitic bonds. The sp^2 sites forming p-bonded clusters, as the carbon concentration increases, tends to stabilize the alloys and to relax the amorphous network by decreasing the tetrahedral coordination and adding some medium-range order to the normal sp^3 short range order. In addition, it was found a smooth and a roughness over an area of 10 μm × 10 μm with a defect on the surface due to a formation of clusters although of the films deposition. Finally, the conductivity of the films decreases with the increase of the carbon concentration, view the increase of the defect density. Therefore, we find that the better passivation is obtained to a cleaning a 5% of carbon.

ACKNOWLEDGEMENTS

The authors want to thank all their colleagues for valuable activities and discussions especially Khelifati Nabil for support at QSSPC measurements. This work was supported by the National Research Fund of DG-RSDT / MESRS from Algeria (FNR11_13 UDTS).

REFERENCES

1. Qayyum A, et al. Growth and properties of glow-discharge hydrogenated amorphous silicon-carbon alloys from silane-propane mixtures. Thin Solid Films. 1988;164:221-226.
2. Patil SB, et al. Photoluminescent, wide-bandgap a-SiC: H alloy films deposited by Cat-CVD using acetylene. Thin Solid Films. 2003;430:244-248.
3. Magafas L, et al. Optimization of Al/a-SiC:H optical sensor device by means of thermal annealing. Microelectronics. 2007;38:1196-1201.
4. Pereyra I, et al. Thick SiOxNy and SiO_2 films obtained by PECVD technique at low temperature. Thin Solid Films. 1998;332:40-45.
5. Li SX, et al. Hydrogenated amorphous silicon-carbide thin films with high photo-sensitivity prepared by layer-by-layer hydrogen annealing technique. Chen Appl Surf Sci. 2013;270:287-291.
6. Rajab SM, et al. Effect of the thermal annealing on the electrical and physical properties of SiC thin films produced by RF magnetron sputtering. Thin Solid Films. 2006;515:170-175.
7. Cathrine Y, et al. Reactive plasma deposited $Si_xC_yH_z$ films. Thin Solid Films. 1979;60:193-200.
8. Wieder H, et al. Vibrational spectrum of hydrogenated amorphous Si-C films. Phys Stat Sol. 1979:99.
9. Munekata H, et al. White photoluminescence of amorphous silicon-carbon alloy prepared by glow-discharge decomposition of tetramethylsilane. Appl Phys Lett. 1980;37:536.
10. Solomon I, et al. Band structure of carbonated amorphous silicon studied by optical, photoelectron, and x-ray spectroscopy. Phy Rev. 1988;38.
11. Solomon I, et al. Selective low-power plasma decomposition of silane-methane mixtures for the preparation of methylated amorphous silicon. Phys Rev. 1988.
12. https://assets.tue.nl/fileadmin/content/faculteiten/tn/PMP/SolarLab_documents/Thesis_dingemans_final.pdf
13. Huong PV, et al. Characterization of methylated amorphous silicon by IR and Raman spectroscopies. Mat Sci Eng. 1991;9:249-252.
14. Kobzev AP, et al. Investigation of light element contents in subsurface layers of silicon. Vacuum. 2009;83:124-126
15. Habibuddin Shaik H, et al. Influence of Si–C bond density on the properties of a-Si1−xCx thin films. J Appl Surf Sci. 2012;258:2989-2996.
16. Van Swaaij RACMM, et al. Local structure and bonding states in a-Si1-xCx:H. Appl Phys.76;251:1994.
17. Huong PV, Characterization of methylated amorphous silicon by IR and Raman spectroscopies. Mater Sci and Eng. 1991;249.
18. Kobzev AP, et al. Investigation of light element contents in subsurface layers of silicon. Vaccum. 2009;83:S124-S126.
19. Fraga MA et al. Nitrogen doping of SiC thin films deposited by RF magnetron sputtering. Journal of Materials Science Materi-

als in Electronics. 2008;19:835-884.

20. Stiropoulos J, et al. Optical properties and structure of $Si_{1-x}C_x$: H alloys. Non Cryst Solids. 1987.
21. Solomon I, et al. Amorphous silicon–carbon alloys: a promising but complex and very diversified series of materials. Applied Surface Science. 2001;184:3-7.
22. Chauvet O, et al. Paramagnetic defects in SiC-based materials. Mater Sci. 1992;83:1201.
23. Ambrosone G, et al. Structural and electrical properties of nanostructured silicon carbon films. Energy Procedia. 2010;2:3-7.
24. Gaufres A, et al. Passivating properties of hydrogenated amorphous silicon carbide deposited by PECVD technique for photovoltaic applications. Energy Procedia. 2013;38:823-832.